Research Square

Preprints are preliminary reports that have not undergone peer review.
They should not be considered conclusive, used to inform clinical practice,
or referenced by the media as validated information.

Ocular Involvement in Cat Scratch Disease: Clinical Spectrum and Retinal Structural Changes with Multimodal Imaging

Mehmet Sengul[1]

mehmetsengulbeyoglu@gmail.com

Beyoglu Goz Egitim ve Arastirma Hastanesi

Cigdem Altan[1]

Beyoglu Goz Egitim ve Arastirma Hastanesi

Burcu Kemer Atik[1]

Beyoglu Goz Egitim ve Arastirma Hastanesi

Berru Yargi Ozkocak[1]

Beyoglu Goz Egitim ve Arastirma Hastanesi

Berna Basarir[2]

Eye Protection Foundation, Bayrampasa Eye Hospital,

Research Article

Keywords: Cat scratch disease, ocular bartonellosis, retinal infiltrate, neuroretinitis, retinal arterial occlusion

Posted Date: October 18th, 2026

DOI: https://doi.org/10.21203/rs.3.rs-11178927/v1

License: This work is licensed under a Creative Commons Attribution 4.0 International License.
Read Full License

Additional Declarations: No competing interests reported.

Abstract

Purpose: To characterize the clinical phenotypes and multimodal imaging findings of ocular bartonellosis, evaluate associated structural retinal changes, and assess visual outcomes.

Methods: Clinical records of consecutive patients with clinically diagnosed ocular bartonellosis supported by documented *Bartonella henselae* seropositivity and followed at a tertiary referral center between January 2010 and January 2025 were retrospectively reviewed. Demographic and systemic characteristics, ocular findings, multimodal imaging findings, treatment, and visual outcomes were evaluated.

Results: Thirty-six eyes of 29 patients were included. Mean age at presentation was 38.8 ± 13.1 years and mean follow-up was 9.4 ± 8.4 months. Neuroretinitis was observed in 23 eyes (63.8%), papillitis in six (16.7%), isolated superficial retinal infiltrates in seven (19.4%), and retinal arterial occlusion in four (11.1%). After resolution of superficial retinal infiltrates, four eyes showed focal inner retinal atrophy and localized retinal nerve fiber layer defects. Mean best-corrected visual acuity improved from 0.41 ± 0.37 at presentation to 0.75 ± 0.26 at final follow-up ($p < 0.001$). Poor final visual acuity (≤0.5) was observed in seven eyes and was mainly associated with optic disc atrophy and retinal nerve fiber layer thinning.

Conclusion: Ocular bartonellosis may present with diverse posterior segment manifestations. Multimodal imaging may demonstrate persistent focal inner retinal atrophy and localized retinal nerve fiber layer defects after clinical resolution of superficial retinal infiltrates. Poorer visual outcomes were mainly associated with optic nerve atrophy.

Key Message

What is known

Ocular cat scratch disease may cause a broad spectrum of posterior segment manifestations, most commonly neuroretinitis and retinal infiltrates.

What is new

Longitudinal multimodal imaging demonstrated persistent focal inner retinal atrophy and localized retinal nerve fiber layer defects at the sites of clinically resolved superficial retinal infiltrates. These structural changes could remain detectable despite the absence of clinically visible residual scarring.

Introduction

Cat scratch disease (CSD) is a systemic zoonotic infection caused by the Gram-negative bacterium *Bartonella henselae*. Humans primarily acquire the infection through interactions with cats, particularly via scratches or bites from kittens [1, 2]. The cat flea *(Ctenocephalides felis)* acts as the primary vector for *Bartonella henselae* and plays a key role in its transmission among cats [3].

Cat scratch disease typically begins with cutaneous involvement at the site of the bite or scratch. Regional lymphadenopathy usually develops within the first week following the skin lesion and may be accompanied by flu-like symptoms such as fever, malaise, and fatigue [2]. In addition to its typical presentation, cat scratch disease may manifest with atypical systemic involvement, including hepatosplenic, ocular, neurologic, dermatologic, hematologic, musculoskeletal, cardiac, renal, and pulmonary involvement [4].

Ocular involvement is the most common atypical manifestation [2]. The most frequent ocular presentation is Parinaud oculoglandular syndrome, characterized by granulomatous conjunctivitis and ipsilateral preauricular lymphadenopathy [2, 5]. Other ocular manifestations include neuroretinitis, retinitis, choroiditis, retinochoroiditis, branch retinal artery and vein occlusion, and serous retinal detachment [5]. Although the clinical spectrum of ocular CSD is well recognized, the structural retinal changes that may persist after clinical resolution have not been well characterized. Therefore, this study aimed to characterize the clinical phenotypes and multimodal imaging findings of ocular CSD, evaluate associated structural retinal changes, and assess visual outcomes during follow-up.

Materials and Methods

This retrospective study included patients with ocular bartonellosis followed at the Uvea Department of Beyoglu Eye Training and Research Hospital, University of Health Sciences Türkiye, a tertiary ophthalmic referral center, between January 2010 and January 2025. Inclusion criteria were a clinical diagnosis of ocular bartonellosis by a uveitis specialist based on compatible ocular findings, documented *Bartonella henselae* seropositivity by enzyme-linked immunosorbent assay (ELISA), and a minimum follow-up of three months with at least two documented visits. Patients with suspected ocular bartonellosis but without documented *B. henselae* serologic results were excluded. The study protocol was approved by the Institutional Review Board of the University of Health Sciences Istanbul Training and Research Hospital Scientific Research Ethics Committee (27/09.01.2026) and the study was also conducted in accordance with the principles of the Declaration of Helsinki.

Serologic testing for *Bartonella henselae* was performed by ELISA at external laboratories, as Bartonella serologic testing was not available on site at our tertiary ophthalmic referral center. Because of the retrospective design of the study and the use of different external laboratories, original laboratory reports and assay-specific quantitative antibody values, index values, and positivity thresholds were not consistently available for retrospective review. Therefore, *B. henselae* IgG and IgM results were extracted from the contemporaneous medical records and recorded qualitatively as positive or negative.

Demographic data, symptoms prior to ocular presentation, history of cat contact or scratches, follow-up duration, routine analysis of complete blood count, biochemistry, acute phase reactants, syphilis serology, hepatitis markers, and HIV enzyme-linked immunosorbent assay (ELISA); best-corrected visual acuity (BCVA) via Snellen chart, intraocular pressure measurements via Goldmann applanation

tonometry, anterior and dilated posterior segment examination findings at initial presentation and during follow-up and treatments were recorded and analyzed.

Posterior segment involvement was categorized into three mutually exclusive clinical phenotypes: neuroretinitis, papillitis, and isolated superficial retinal infiltrates. Neuroretinitis was defined as optic disc edema associated with a complete or incomplete macular star either at presentation or developing during follow-up. Papillitis was defined as optic disc edema without development of a macular star throughout follow-up. Eyes with superficial retinal infiltrates in the absence of neuroretinitis or papillitis were classified as having isolated superficial retinal infiltrates. Retinal arterial occlusions were recorded separately.

In addition, posterior segment findings were documented using color fundus photography (Topcon Corporation, Tokyo, Japan) and spectral domain optical coherence tomography (OCT), blue reflectance imaging, fundus fluorescein angiography (FFA), and peripapillary retinal nerve fiber layer (RNFL) thickness, central macular thickness (Spectralis; Heidelberg Engineering, Heidelberg, Germany). Automated static perimetry (Humphrey Systems, Inc., Dublin, CA, USA) was also performed in patients with concomitant arterial occlusion.

Structural retinal changes at the sites of previously documented superficial retinal infiltrates were evaluated during follow-up. Focal inner retinal atrophy was considered present when follow-up OCT demonstrated localized thinning of the inner retinal layers corresponding to the site of a clinically resolved infiltrate. Localized RNFL defects were assessed on blue-reflectance imaging when available.

Statistical analyses were performed using IBM SPSS Statistics for Windows, version 22.0 (IBM Corp., Armonk, NY, USA). The normality of data distribution was assessed using the Shapiro–Wilk test. Paired continuous variables were compared using the paired-samples t-test for normally distributed data and the Wilcoxon signed-rank test for non-normally distributed data. Comparisons of continuous variables between independent groups were performed using the independent-samples t-test or the Mann–Whitney U test, as appropriate. Categorical variables were compared using the chi-square test or Fisher's exact test, as appropriate. A p-value < 0.05 was considered statistically significant.

Results

In total, 36 eyes of 29 patients were included in the study. There were 15 females (51.7%) and 14 males (48.3%). The mean age at presentation was 38.8 ± 13.1 years (range: 17–63 years), and the mean follow-up duration was 9.4 ± 8.4 months (range: 3–39 months). No patients included in the study exhibited immunodeficiency. Systemic comorbidities included hypothyroidism in two patients and hypertension in one patient. Toxoplasma IgG seropositivity was detected in four patients (13.8%), and elevated ACE levels were noted in three patients (10.3%). Syphilis serology (VDRL and TPHA) and HIV testing were negative in all patients. The demographic characteristics and relevant clinical data of the subjects are summarized in Online Resource 1.

A prior history of cat contact was noted in 20 patients (68.9%). Regarding systemic involvement, flu-like symptoms were observed in three patients (10.3%; lasting 1, 1.5, and 2 weeks), and severe headaches in three patients (10.3%). Lymphadenopathy was observed in five patients (17.2%), including submandibular lymphadenopathy in two patients (6.9%), cervical + preauricular lymphadenopathy in two patients (6.9%), and isolated preauricular lymphadenopathy in one patient (3.4%). The initial presentation in all patients was reduced or blurred vision. Additionally, one patient (3.4%) reported eye pain, and two patients (6.9%) presented with right-sided visual field loss. In seven patients (24.1%) the involvement was bilateral.

The mean BCVA at presentation was 0.41 ± 0.37. BCVA was ≥ 0.7 in 13 eyes (1.0 in 6 eyes), 0.1 ≤ BCVA ≤ 0.3 in 15 eyes, and < 0.1 in eight eyes at first visit. The mean IOP was 14.3 ± 3.4 mmHg (range: 7–22 mmHg). One patient presented with marked anterior chamber reaction (+ 4 cells with hypopyon), and two patients had + 1 anterior chamber cells, whereas the anterior chambers of the remaining patients were quiescent; vitreous was quiescent in 21 eyes (58.3%), while grade 1 + vitritis was documented in eight eyes (22.2%) and grade 2 + vitritis in seven eyes (19.4%).

Neuroretinitis was observed in 23 eyes (63.8%), papillitis in six eyes (16.7%), and isolated superficial retinal infiltrates in seven eyes (19.4%). Superficial retinal infiltrates were observed in 21 eyes (58.3%), including nine eyes with neuroretinitis, five with papillitis, and seven with isolated superficial retinal infiltrates. Retinal arterial occlusion was observed in four eyes (11.1%); two of these eyes had papillitis with superficial retinal infiltrates, one had isolated superficial retinal infiltrates, and one had neuroretinitis with superficial retinal infiltrates.

In addition, one eye with neuroretinitis (Case 4) exhibited periorbital inflammation, marked anterior chamber inflammation (+ 4 cells with hypopyon), optic disc edema, subretinal fluid, and a T-sign on orbital ultrasound, consistent with a posterior scleritis-like presentation. The patient was positive for both Bartonella henselae IgM and IgG.

Fundus fluorescein angiography was available in 20 eyes of 16 patients. Optic disc leakage was present in 15 eyes (75%). Early hypofluorescence followed by late hyperfluorescence at the margins of superficial retinal infiltrates was observed in four eyes (20%), while persistent hypofluorescence from early to late phases was observed in two eyes (10%). Arterial filling delay or occlusion was observed in four eyes (20%), and perivascular staining in one eye (5%).

At the initial visit, macular star was present in 17 eyes (47.2%), seven of which were incomplete. During follow-up, macular star was present in six eyes (16.6%), bringing the total to 23 eyes (63.8%). The mean time to macular star development was 7.3 ± 1.8 days. Macular star resolution time could be evaluated in 14 eyes, with a mean duration of 4.5 ± 2.3 weeks (range: 1–9 weeks). In eight eyes, incomplete macular star persisted at the final visit, with follow-up durations ranging from 3 to 4 months. Initial BCVA in eyes with neuroretinitis was 0.24 ± 0.20, whereas it was 0.68 ± 0.36 in the remaining eyes, and this difference was statistically significant ($p < 0.001$). There was no bilateral macular star involvement.

Serum *Bartonella henselae* IgG was positive in all patients, while IgM was positive in 23 patients (79.3%). All patients received oral antibiotic therapy with doxycycline 200 mg/day (Tetradox 100 mg, Teva Pharmaceuticals, Türkiye) for 4–6 weeks, either as monotherapy or in combination with rifampin 300 mg/day (Rifcap 300 mg, Koçak Pharmaceuticals, Türkiye) for 4–6 weeks or azithromycin (Azitro 500 mg, Deva Pharmaceuticals, Türkiye) for nine days. Patients with anterior segment inflammation received topical prednisolone acetate (Pred Forte 1%, Allergan Pharmaceuticals, Ireland) and cyclopentolate hydrochloride (Sikloplejin 1%, Abdi İbrahim Pharmaceuticals, Türkiye) eye drops. Additionally, 21 patients (72.4%) were administered oral steroid therapy (Methylprednisolone; Prednol 16 mg, Gensenta, Türkiye) at doses 24–32 mg/day, gradually tapered by usually 8 mg/day per week, in conjunction with antibiotic therapy, based on the resolution of optic nerve edema, and one patient (Case 4) received intravenous pulse steroid (1 g/day methylprednisolone) treatment.

All patients demonstrated regression of clinical findings following treatment. Peripapillary retinal nerve fiber layer thickness significantly decreased from baseline (188.6 ± 80.5 μm) to the final visit (92.3 ± 22.0 μm) ($p < 0.001$). Similarly, central macular thickness showed a significant reduction from baseline (401.4 ± 197.6 μm) to the final visit (252.9 ± 28.9 μm) ($p < 0.001$). Macular edema was observed in 23 eyes (63.9%) at baseline, including subretinal fluid in 16 eyes (44.4%), intraretinal fluid in three eyes (8.3%), and combined subretinal and intraretinal fluid in four eyes (11.1%). Hyperreflective dots were detected in 22 eyes (61.1%), coexisting with macular edema in 16 eyes (44.4%).

Among the 21 eyes with superficial retinal infiltrates, 15 eyes (71.4%) were located in the posterior pole and six eyes (28.6%) in the peripheral retina. Optical coherence tomography through the lesion was available in seven eyes with posterior pole involvement. Blue-reflectance imaging and FFA were available in nine and 13 eyes, respectively, with superficial retinal infiltrates. Following resolution of superficial retinal infiltrates, four eyes demonstrated focal inner retinal atrophy and localized RNFL defects without residual scarring (Figs. 1 and 3). In two eyes with concomitant arterial occlusion, structural changes attributable specifically to the previous infiltrates could not be reliably assessed because of coexisting inner retinal atrophy.

The mean BCVA at presentation was 0.41 ± 0.37, improving to 0.75 ± 0.26 at the final visit ($p < 0.001$). At the final visit, BCVA was ≥ 0.7 in 26 eyes (72.2%) (1.0 in 13 eyes, 36.1%), 0.1 ≤ BCVA ≤ 0.6 in 10 eyes (27.8%) (0.6 in three eyes, 0.5 in two eyes, 0.4 in one eye, 0.2 in three eyes, and 0.1 in one eye), and no eye had < 0.1. Of the seven eyes with final BCVA ≤ 0.5, five eyes (71.4%) presented with neuroretinitis, one had persistent incomplete macular star at the final visit (follow-up: 3 months), and six eyes (85.7%) showed optic atrophy at the final visit. Clinical and imaging details of these seven eyes are summarized in Table 1.

Table 1
Clinical and imaging features of eyes with final BCVA ≤ 0.5

Case Number	Eye	Initial BCVA	Final BCVA	Ocular involvement	Persistent macular star	RNFL (μm)	Optic atrophy	Follow-up (months)
1	R	0.16	0.1	NR	Yes	106	No	3
2	L	CF 50 cm	0.2	Papillitis + SRI	No	72	Yes	8
10	L	CF 1 m	0.4	NR + SRI	No	55	Yes	39
19	L	0.16	0.5	SRI + BRAO	No	70	Yes	14
20	R	0.1	0.5	NR + SRI + BRAO	No	60	Yes	22
22	L	0.16	0.2	NR	No	57	Yes	22
26	L	CF 1 m	0.2	NR	No	43	Yes	4

BCVA: Best corrected visual acuity; RNFL: Peripapillary retinal nerve fiber layer; CF: Counting fingers; NR: Neuroretinitis; SRI: Superficial retinal infiltrate; BRAO: Branch retinal artery occlusion

Discussion

In this study, ocular bartonellosis demonstrated a broad spectrum of posterior segment manifestations, with neuroretinitis and superficial retinal infiltrates representing the predominant clinical findings. Although visual outcomes were generally favorable, poorer final visual acuity was mainly associated with optic nerve atrophy. Importantly, multimodal imaging demonstrated persistent focal inner retinal atrophy and localized RNFL defects at the sites of clinically resolved superficial retinal infiltrates, suggesting that apparent clinical resolution may be accompanied by residual structural retinal changes.

According to the literature, the mean age of patients with CSD is generally reported to be pediatric and adolescent age groups [1, 2]. In contrast, the mean age of our study was 38.8 ± 13.1 (17–63) years. However, several studies have also reported a higher mean age, exceeding 20 years [6, 7]. Wilner et al. [8] analyzed 86 patients with ocular CSD (107 eyes) identified from a national surveillance cohort of 3,222 patients with CSD and reported a mean age of 35.1 ± 14.2 years, representing one of the largest ocular CSD cohorts documented in the literature. The role of cat contact in the transmission of CSD has been well established in the literature [1, 2, 9, 10]. In our study, a history of cat contact was identified in 68.9% of patients. In contrast, cat exposure has been reported at higher rates in earlier series, including 99% in 1,200 patients [2], 93% in 160 patients [11] with CSD, and 86% in 84 patients [8] with ocular CSD. *Bartonella henselae* can also be transmitted by cat fleas and other arthropod vectors [3]. This variability suggests that a history of direct cat contact may support the diagnosis but is not invariably present in ocular

bartonellosis. Accordingly, in patients without a known history of cat exposure, the diagnosis requires integration of the ocular phenotype, clinical assessment, serologic findings, and evaluation for relevant alternative causes rather than reliance on exposure history alone.

Neuroretinitis is the most common posterior segment manifestation of CSD [2, 5, 12, 13] and *Bartonella henselae* is the most frequently identified etiologic agent of neuroretinitis [13, 14]. Suhler et al. conducted serological testing in 14 out of 18 patients diagnosed with neuroretinitis and found that 9 of these patients tested positive for Bartonella serology [14].

Clinically, neuroretinitis typically presents with unilateral, painless visual loss. The primary pathophysiology is inflammation of the optic disc head and leakage of vascular contents into the outer plexiform layer of peripapillary retina. After serum reabsorption, the remaining lipid exudates, due to the radial configuration of the outer plexiform layer, appear as a star-shaped configuration [15]. However, macular star formation is not specific to neuroretinitis. It may occur one to two weeks after disc edema, therefore, patients presenting with papillitis should be re-examined for subsequent macular star formation [16]. Disc edema begins to resolve within two weeks, and the process may extend up to 12 weeks. Macular star begins to resolve within 1 month, but it may be necessary to wait 6–12 months for complete resolution [12]. The sequential development and regression of macular star following optic disc edema are demonstrated in a patient (Case 22) in Fig. 2.

In our study, neuroretinitis was observed in 23 eyes (63.8%). Macular star was present in 17 eyes (47.2%) at presentation including seven eyes with an incomplete star configuration and developed in six additional eyes (16.6%) during follow-up, making neuroretinitis the most common posterior segment manifestation. Similar frequencies have been reported in prior ocular Bartonella series, with neuroretinitis observed in 28 (45%) of 62 eyes [17] and 74 (69%) of 107 eyes [8]. The delayed appearance of macular exudates in several eyes in our cohort is consistent with recent observations by Rajan et al., who noted macular star in 25 of 33 eyes (75.8%) with CSD-associated neuroretinitis, including 15 eyes (45.5%) with a complete star and 10 eyes (30.3%) with an incomplete star, while eight eyes (24.2%) lacked macular exudates at presentation but developed them during the disease course [18].

Retinal and choroidal infiltration may also be observed among posterior segment manifestations. In our study, superficial retinal infiltrates were identified in 21 eyes (58.3%), constituting the second most common posterior segment manifestation (coexisting with neuroretinitis in nine eyes [25.0%], with papillitis in five eyes [13.9%], and isolated in seven eyes [19.4%]). Solley et al. reported discrete white retinal or choroidal lesions in 29 of 35 eyes (83%), the most frequent posterior segment finding in their CSD cohort, eight with neuroretinitis (23%) and 12 isolated (34%) [19].

Superficial retinal infiltrates in ocular CSD should be distinguished from the retinal infiltrates observed in Behçet's uveitis. Retinal infiltrates in CSD tend to resolve gradually over weeks [20, 21] in contrast to Behçet disease, where they resolve rapidly and spontaneously within days [22]. Residual scarring may

remain following resolution in CSD [13, 19, 23] and structural sequelae have also been reported in Behçet's uveitis [22, 24]. In their multimodal imaging–based evaluation of Behçet disease, Tugal-Tutkun et al. [25] demonstrated that superficial retinal infiltrates may regress rapidly on clinical examination; however, OCT often reveals residual structural sequelae, predominantly involving the inner retinal layers, including focal atrophy and localized retinal nerve fiber layer defects. Similarly, in our cohort of ocular bartonellosis, multimodal imaging demonstrated focal inner retinal atrophy and localized RNFL defects at the sites of clinically resolved superficial retinal infiltrates (Fig. 3). To our knowledge, these persistent structural sequelae have not previously been reported in ocular CSD.

Posterior segment manifestations can also present with vascular involvement such as retinal artery and vein occlusions [8, 19, 26]. The clinical consequences of vascular involvement depend on its location. Peripheral involvement may cause blurred vision or a corresponding visual field defect, whereas central vascular involvement may result in severe visual loss, including no light perception, and neovascular glaucoma [27]. Retinal artery occlusion occurred in four eyes in our cohort, frequently in association with superficial retinal infiltrates (Fig. 4). Notably, retinal infiltrates were spatially adjacent to the occluded arterial segment in two eyes, suggesting a potential local mechanical or inflammatory contribution. Solley et al. [19] stated that this could be caused by the mechanical effect of the retinal infiltrate adjacent to the artery, and they also suggested that *Bartonella henselae* might contribute to the occlusion by causing endothelial damage, stimulating thrombogenic mediators, and subsequently leading to vascular obstruction. It is well-known that *Bartonella henselae* exhibits an affinity for the endothelium [28].

There is no consensus on the antibiotic treatment of CSD. Bartonella spp. have been shown to be susceptible to amoxicillin, third-generation cephalosporins, tetracyclines, macrolides, rifampin, co-trimoxazole, and aminoglycosides [29]. Although the only double-blind study in the literature on the treatment of CSD with antibiotics is with azithromycin, there is still no current recommendation for immunocompetent patients with CSD due to its self-limited nature, as well as concerns such as adverse drug reactions and the development of resistant flora [30]. Oral combination therapy with doxycycline and rifampin is recommended for the treatment of neuroretinitis associated with CSD [30, 31]. In our cohort, all patients received doxycycline, either as monotherapy or in combination with rifampin or azithromycin. Systemic corticosteroids were administered to 22 patients (76%), including oral corticosteroids in 21 patients and combined oral and intravenous pulse therapy in one patient with posterior scleritis, while seven patients were managed without systemic steroids. In their study of 107 eyes, Wilner et al. [8] found that eyes with good initial visual acuity (VA) could be closely monitored without having to treat with antibiotics. They also showed that combination therapy with systemic antibiotics and corticosteroids resulted in a significantly greater improvement in VA than antibiotic treatment alone in patients with moderate to severe visual loss at presentation.

Overall visual prognosis in ocular bartonellosis is generally favorable. In our cohort, final BCVA was ≤ 0.5 in 7 eyes (19.4%), and no eyes had a final BCVA < 0.1. Similarly, severe visual loss has been reported infrequently in previous series. Wilner et al. reported that severe visual loss (VA ≤ 20/200) occurred in 6%

of 79 eyes at final follow-up [8]. Chi et al. found that severe visual loss (VA ≤ 20/200) occurred in 5.7% of 53 eyes [17], while Curi et al. reported that 13.5% of 37 eyes presented with VA worse than 20/200 [32]. Poor visual outcomes in our cohort were primarily associated with optic disc pallor. Six of seven eyes (85.7%) with a final BCVA ≤ 0.5 demonstrated optic pallor at the final visit. Peripapillary retinal nerve fiber layer thinning was present in all eyes with optic pallor. The remaining eye, which lacked both optic pallor and RNFL thinning, had a short follow-up duration (3 months) and exhibited a persistent incomplete macular star, raising the possibility of incomplete structural and functional recovery. These observations suggest that permanent optic nerve injury is closely associated with poorer visual outcomes in ocular bartonellosis.

This study has several limitations. Its retrospective design and relatively small sample size may limit the generalizability of the findings. In addition, OCT scans traversing the retinal lesions, as well as multimodal imaging, particularly blue reflectance imaging and visual field analysis, were not available for all patients after lesion resolution. Treatment modalities were not compared, as all patients were managed according to the institutional practice pattern. Furthermore, this was a single-center study involving a relatively homogeneous patient population, which may further limit external generalizability.

An additional limitation was the non-centralized nature of *B. henselae* serologic testing. Because testing was performed by ELISA at different external laboratories, original assay reports, quantitative antibody values, assay-specific index values, and positivity thresholds could not be consistently retrieved. Serologic data were therefore limited to qualitative IgG and IgM results documented in the medical records. In particular, IgG positivity in the absence of IgM cannot reliably distinguish active infection from previous exposure. Therefore, serologic findings were interpreted as supportive rather than confirmatory, and the diagnosis of ocular bartonellosis was based on the combination of a compatible ocular phenotype, specialist clinical assessment, serologic support, and exclusion of relevant alternative diagnoses.

Conclusion

Ocular bartonellosis may present with various posterior segment manifestations. A detailed history of cat exposure should be obtained in all suspected cases to facilitate diagnosis; however, a history of direct cat contact is not mandatory. In young patients presenting with retinal arterial occlusion, ocular bartonellosis should also be considered in the differential diagnosis. Although retinal infiltrates may resolve clinically, optical coherence tomography may reveal persistent focal inner retinal atrophy and localized retinal nerve fiber layer defects, reflecting residual structural damage.

Declarations

Disclosures:

None of the authors has any conflict of interest to disclose.

Funding

The authors received no funding for this work.

Competing Interests:

The authors have no relevant financial or non-financial interests to disclose.

Ethics Approval:

The study was approved by the Non-Interventional Clinical Research Ethics Committee of the University of Health Sciences Istanbul Training and Research Hospital (Decision No. 27, January 9, 2026) and was conducted in accordance with the principles of the Declaration of Helsinki.

Funding:

No.

Author Contribution

M.S. contributed to the study conception and design, data collection, analysis and interpretation of the data, and preparation of the first draft of the manuscript. C.A. contributed to the study conception and design, interpretation of the data, supervision, and critical revision of the manuscript. B.K.A., B.Y.O., and B.B. contributed to data interpretation and critical revision of the manuscript. All authors read and approved the final manuscript.

Acknowledgements:

None.

Data Availability

The data that support the findings of this study are available from the corresponding author upon reasonable request.

References

1. Zangwill KM, Hamilton DH, Perkins BA, Regnery RL, Plikaytis BD, Hadler JL, et al. Cat scratch disease in Connecticut. Epidemiology, risk factors, and evaluation of a new diagnostic test. N Engl J Med. 1993;329(1):8–13. doi:10.1056/NEJM199307013290102 PubMed PMID: 8505963.

2. Carithers HA. Cat-scratch disease. An overview based on a study of 1,200 patients. Am J Dis Child. 1985;139(11):1124–33. doi:10.1001/archpedi.1985.02140130062031 PubMed PMID: 4061408.
3. Chomel BB, Kasten RW, Floyd-Hawkins K, Chi B, Yamamoto K, Roberts-Wilson J, et al. Experimental transmission of Bartonella henselae by the cat flea. J Clin Microbiol. 1996;34(8):1952–6. doi:10.1128/jcm.34.8.1952-1956.1996 PubMed PMID: 8818889; PubMed Central PMCID: PMC229161.
4. Florin TA, Zaoutis TE, Zaoutis LB. Beyond cat scratch disease: widening spectrum of Bartonella henselae infection. Pediatrics. 2008;121(5):e1413-1425. doi:10.1542/peds.2007-1897 PubMed PMID: 18443019.
5. Cunningham ET, Koehler JE. Ocular bartonellosis. Am J Ophthalmol. 2000;130(3):340–9. doi:10.1016/s0002-9394(00)00573-0 PubMed PMID: 11020414.
6. Kordick DL, Wilson KH, Sexton DJ, Hadfield TL, Berkhoff HA, Breitschwerdt EB. Prolonged Bartonella bacteremia in cats associated with cat-scratch disease patients. J Clin Microbiol. 1995;33(12):3245–51. doi:10.1128/jcm.33.12.3245-3251.1995 PubMed PMID: 8586710; PubMed Central PMCID: PMC228681.
7. Acar A, Çakar Özdal P, Başarır B, Özdemir Yalçınsoy K, Altan Ç, Budakoğlu Ö. A Case Series of Cat-Scratch Disease with Ocular Manifestations: Clinical Findings and Treatment Approach. Turk J Ophthalmol. 2023;53(4):226–33. doi:10.4274/tjo.galenos.2022.44692 PubMed PMID: 37602640; PubMed Central PMCID: PMC10442748.
8. Habot-Wilner Z, Trivizki O, Goldstein M, Kesler A, Shulman S, Horowitz J, et al. Cat-scratch disease: ocular manifestations and treatment outcome. Acta Ophthalmol (Copenh). 2018;96(4):e524–32. doi:10.1111/aos.13684 PubMed PMID: 29504674.
9. Koehler JE, Glaser CA, Tappero JW. Rochalimaea henselae infection. A new zoonosis with the domestic cat as reservoir. JAMA. 1994;271(7):531–5. doi:10.1001/jama.271.7.531 PubMed PMID: 8301768.
10. Demers DM, Bass JW, Vincent JM, Person DA, Noyes DK, Staege CM, et al. Cat-scratch disease in Hawaii: Etiology and seroepidemiology. J Pediatr. 1995;127(1):23–6. doi:10.1016/S0022-3476(95)70251-2
11. Daniels WB, Macmurray FG. Cat scratch disease; report of one hundred sixty cases. J Am Med Assoc. 1954;154(15):1247–51. doi:10.1001/jama.1954.02940490011003 PubMed PMID: 13151831.
12. Dreyer RF, Hopen G, Gass JD, Smith JL. Leber's idiopathic stellate neuroretinitis. Arch Ophthalmol. 1984;102(8):1140–5. doi:10.1001/archopht.1984.01040030918013 PubMed PMID: 6466174.
13. Reed JB, Scales DK, Wong MT, Lattuada CP, Dolan MJ, Schwab IR. Bartonella henselae neuroretinitis in cat scratch disease. Diagnosis, management, and sequelae. Ophthalmology. 1998;105(3):459–66. doi:10.1016/S0161-6420(98)93028-7 PubMed PMID: 9499776.
14. Suhler EB, Lauer AK, Rosenbaum JT. Prevalence of serologic evidence of cat scratch disease in patients with neuroretinitis. Ophthalmology. 2000;107(5):871–6. doi:10.1016/S0161-

6420(00)00002-6

15. Maitland CG, Miller NR. Neuroretinitis. Arch Ophthalmol. 1984;102(8):1146–50. doi:10.1001/archopht.1984.01040030924014 PubMed PMID: 6466175.
16. Brazis PW, Lee AG. Optic disk edema with a macular star. Mayo Clin Proc. 1996;71(12):1162–6. doi:10.4065/71.12.1162 PubMed PMID: 8945487.
17. Chi SL, Stinnett S, Eggenberger E, Foroozan R, Golnik K, Lee MS, et al. Clinical characteristics in 53 patients with cat scratch optic neuropathy. Ophthalmology. 2012;119(1):183–7. doi:10.1016/j.ophtha.2011.06.042 PubMed PMID: 21959368.
18. Rajan RS, Kuganasan S, Ali NS, Aziz RAA, Mohamed SO. Clinical and imaging characteristics of neuroretinitis secondary to cat scratch disease from tertiary centers in Malaysia: a retrospective study. J Ophthalmic Inflamm Infect. 2025;15(1):96. doi:10.1186/s12348-025-00539-w PubMed PMID: 41273610; PubMed Central PMCID: PMC12748332.
19. Solley WA, Martin DF, Newman NJ, King R, Callanan DG, Zacchei T, et al. Cat scratch disease: posterior segment manifestations. Ophthalmology. 1999;106(8):1546–53. doi:10.1016/S0161-6420(99)90452-9 PubMed PMID: 10442903.
20. Ormerod LD, Skolnick KA, Menosky MM, Pavan PR, Pon DM. Retinal and choroidal manifestations of cat-scratch disease. Ophthalmology. 1998;105(6):1024–31. doi:10.1016/S0161-6420(98)96003-1 PubMed PMID: 9627652.
21. Ksiaa I, Abroug N, Mahmoud A, Zina S, Hedayatfar A, Attia S, et al. Update on Bartonella neuroretinitis. J Curr Ophthalmol. 2019;31(3):254–61. doi:10.1016/j.joco.2019.03.005 PubMed PMID: 31528758; PubMed Central PMCID: PMC6742623.
22. Tugal-Tutkun I, Gupta V, Cunningham ET. Differential diagnosis of behçet uveitis. Ocul Immunol Inflamm. 2013;21(5):337–50. doi:10.3109/09273948.2013.795228 PubMed PMID: 23730816.
23. Carroll DM, Franklin RM. Leber's idiopathic stellate retinopathy. Am J Ophthalmol. 1982;93(1):96–101. doi:10.1016/0002-9394(82)90706-1 PubMed PMID: 6278934.
24. Oray M, Onal S, Bayraktar S, Izgi B, Tugal-Tutkun I. Nonglaucomatous localized retinal nerve fiber layer defects in Behçet uveitis. Am J Ophthalmol. 2015;159(3):475–481.e1. doi:10.1016/j.ajo.2014.11.029 PubMed PMID: 25461299.
25. Tugal-Tutkun I, Ozdal PC, Oray M, Onal S. Review for Diagnostics of the Year: Multimodal Imaging in Behçet Uveitis. Ocul Immunol Inflamm. 2017;25(1):7–19. doi:10.1080/09273948.2016.1205100 PubMed PMID: 27541278.
26. Oray M, Önal S, Koç Akbay A, Tuğal Tutkun İ. Diverse Clinical Signs of Ocular Involvement in Cat Scratch Disease. Turk J Ophthalmol. 2017;47(1):9–17. doi:10.4274/tjo.28009 PubMed PMID: 28182175; PubMed Central PMCID: PMC5282546.
27. Gray AV, Michels KS, Lauer AK, Samples JR. Bartonella henselae infection associated with neuroretinitis, central retinal artery and vein occlusion, neovascular glaucoma, and severe vision loss. Am J Ophthalmol. 2004;137(1):187–9. doi:10.1016/s0002-9394(03)00784-0 PubMed PMID: 14700670.

28. Kirby JE. In vitro model of Bartonella henselae-induced angiogenesis. Infect Immun. 2004;72(12):7315–7. doi:10.1128/IAI.72.12.7315-7317.2004 PubMed PMID: 15557658; PubMed Central PMCID: PMC529148.
29. Maurin M, Raoult D. Antimicrobial susceptibility of Rochalimaea quintana, Rochalimaea vinsonii, and the newly recognized Rochalimaea henselae. J Antimicrob Chemother. 1993;32(4):587–94. doi:10.1093/jac/32.4.587 PubMed PMID: 8288500.
30. Rolain JM, Brouqui P, Koehler JE, Maguina C, Dolan MJ, Raoult D. Recommendations for treatment of human infections caused by Bartonella species. Antimicrob Agents Chemother. 2004;48(6):1921–33. doi:10.1128/AAC.48.6.1921-1933.2004 PubMed PMID: 15155180; PubMed Central PMCID: PMC415619.
31. Bass JW, Freitas BC, Freitas AD, Sisler CL, Chan DS, Vincent JM, et al. Prospective randomized double blind placebo-controlled evaluation of azithromycin for treatment of cat-scratch disease. Pediatr Infect Dis J. 1998;17(6):447–52. doi:10.1097/00006454-199806000-00002 PubMed PMID: 9655532.
32. Curi ALL, Machado D, Heringer G, Campos WR, Lamas C, Rozental T, et al. Cat-scratch disease: ocular manifestations and visual outcome. Int Ophthalmol. 2010;30(5):553–8. doi:10.1007/s10792-010-9389-5 PubMed PMID: 20668914.

Figures

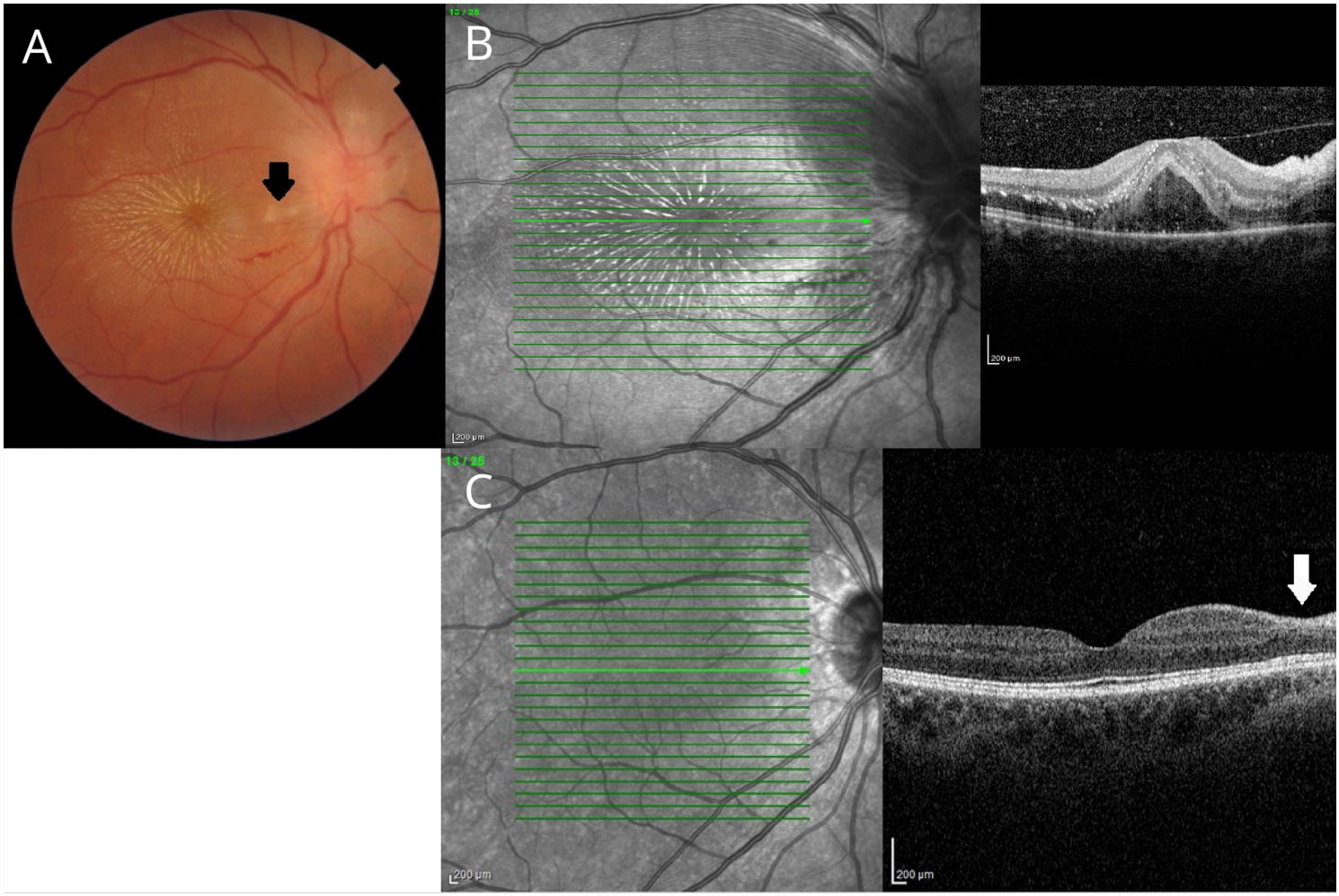


Figure 1

Color fundus photography of Case 11 at presentation shows optic disc edema with blurred margins, a macular star, and a retinal infiltrate in the temporal region of the optic disc (A). Macular OCT B-scan at presentation demonstrates subretinal fluid and hyperreflective material (B). At the final visit (follow-up duration: 38 months), Macular OCT B-scan shows focal inner retinal atrophy at the site of the previous infiltration (white arrow) (C).

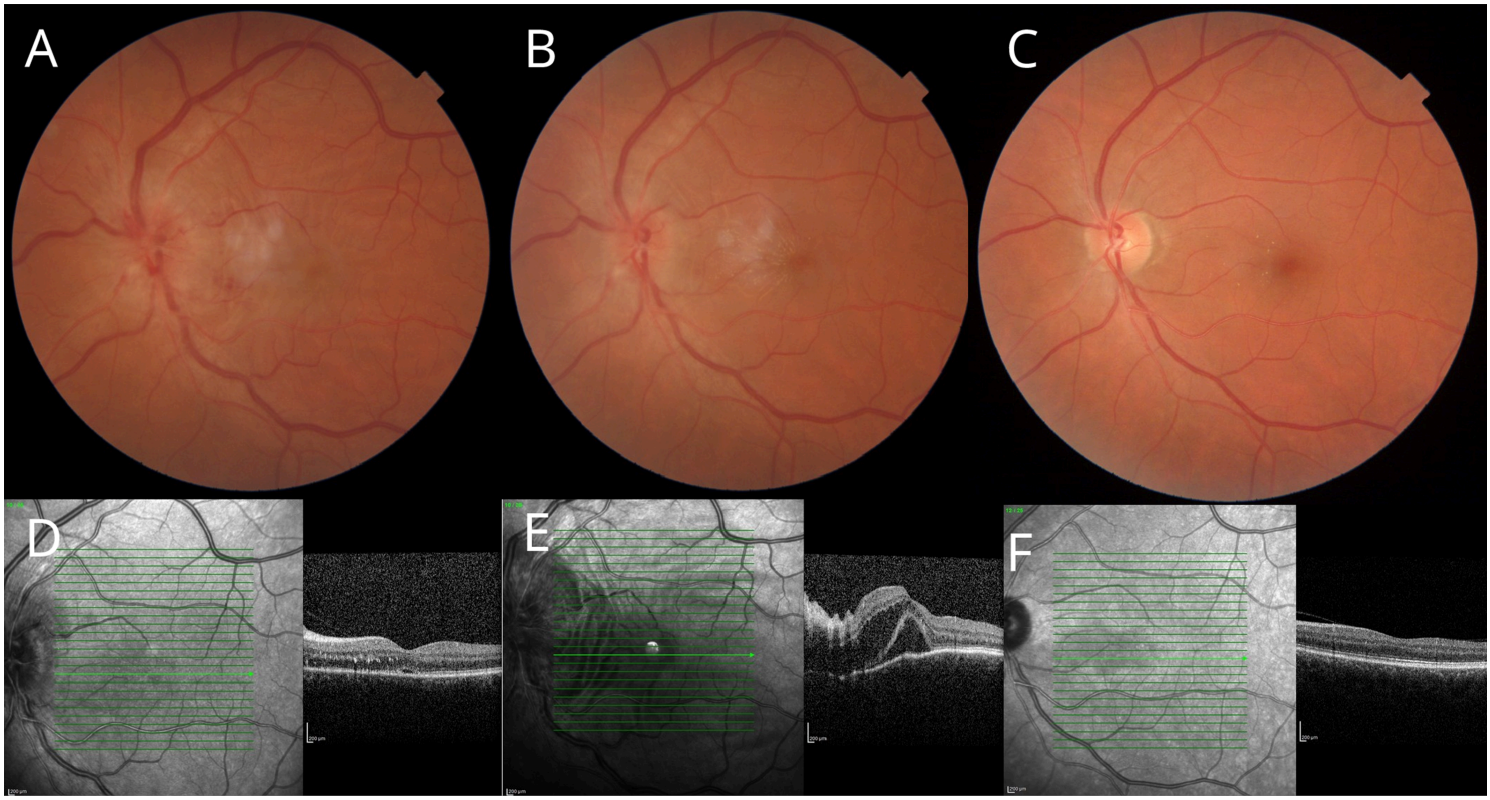


Figure 2

Sequential color fundus photographs of a representative patient (Case 22) with neuroretinitis taken at presentation (A), at day 10 of follow-up (B), and at 4-month follow-up (C). At presentation, optic disc edema with prominent Paton's lines is observed (A). On day 10, partial regression of disc edema with blurred disc margins and persistent hyperemia is evident, along with the development of an incomplete temporal macular star (B). At 4 months, optic disc hyperemia has disappeared, and the incomplete macular star has markedly regressed, leaving only scattered temporal exudates (C). Corresponding macular OCT B-scan imaging obtained at presentation (D), day 10 (E), and month 4 (F) demonstrates hyperreflective exudates at presentation (D), foveal detachment and subretinal fluid at day 10 (E), and resolution of subretinal fluid with restoration of foveal contour at month 4 (F).

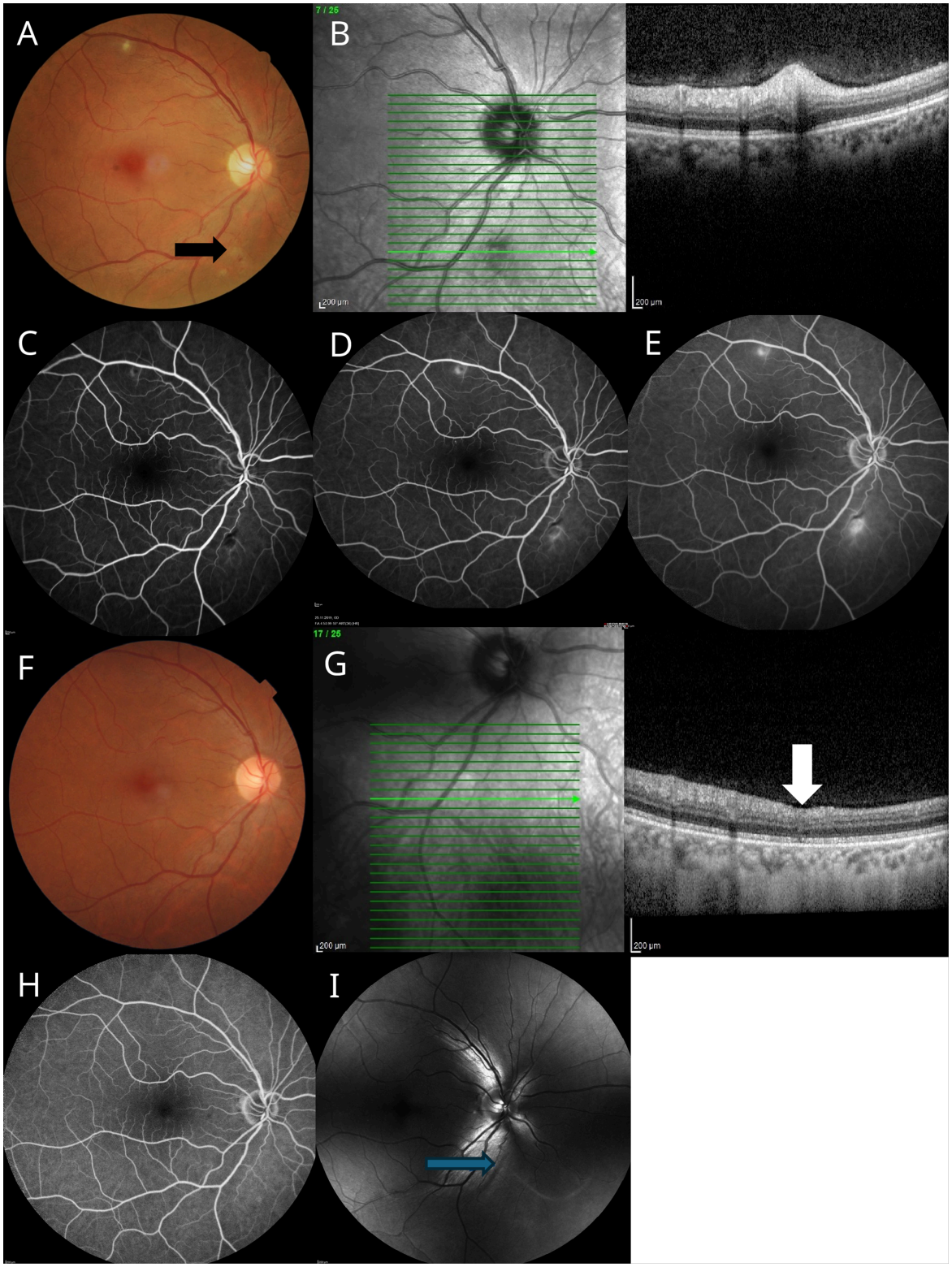


Figure 3

Multimodal imaging of a patient (Case 8) with superficial retinal infiltrates (A–E at presentation; F–I at 24-month follow-up). At presentation, color fundus photography shows a focal superficial retinal infiltrate inferiorly (black arrow) and a second lesion at the distal portion of the superotemporal vascular arcade (A). The corresponding macular OCT B-scan through the inferior lesion demonstrates focal retinal thickening with increased intraretinal reflectivity (B). Early fluorescein angiography (FA) at 40 seconds

shows hypofluorescent areas corresponding to the superficial retinal infiltrates (C). Mid-phase FA at 2 minutes reveals a hypofluorescent core with surrounding hyperfluorescent staining (D). Late-phase FA at 7 minutes demonstrates progressive staining of the superficial infiltrates (E). At the 24-month follow-up, color fundus photography shows complete regression of the infiltrates (F). The corresponding OCT B-scan displays focal inner retinal layer atrophy consistent with structural sequelae (white arrow) (G). Late-phase FA at 7 minutes shows no residual staining or leakage at the sites of the previous infiltrates (H). Blue reflectance imaging demonstrates a focal defect in the nerve fiber layer corresponding to the area of prior infiltration (blue arrow) (I).

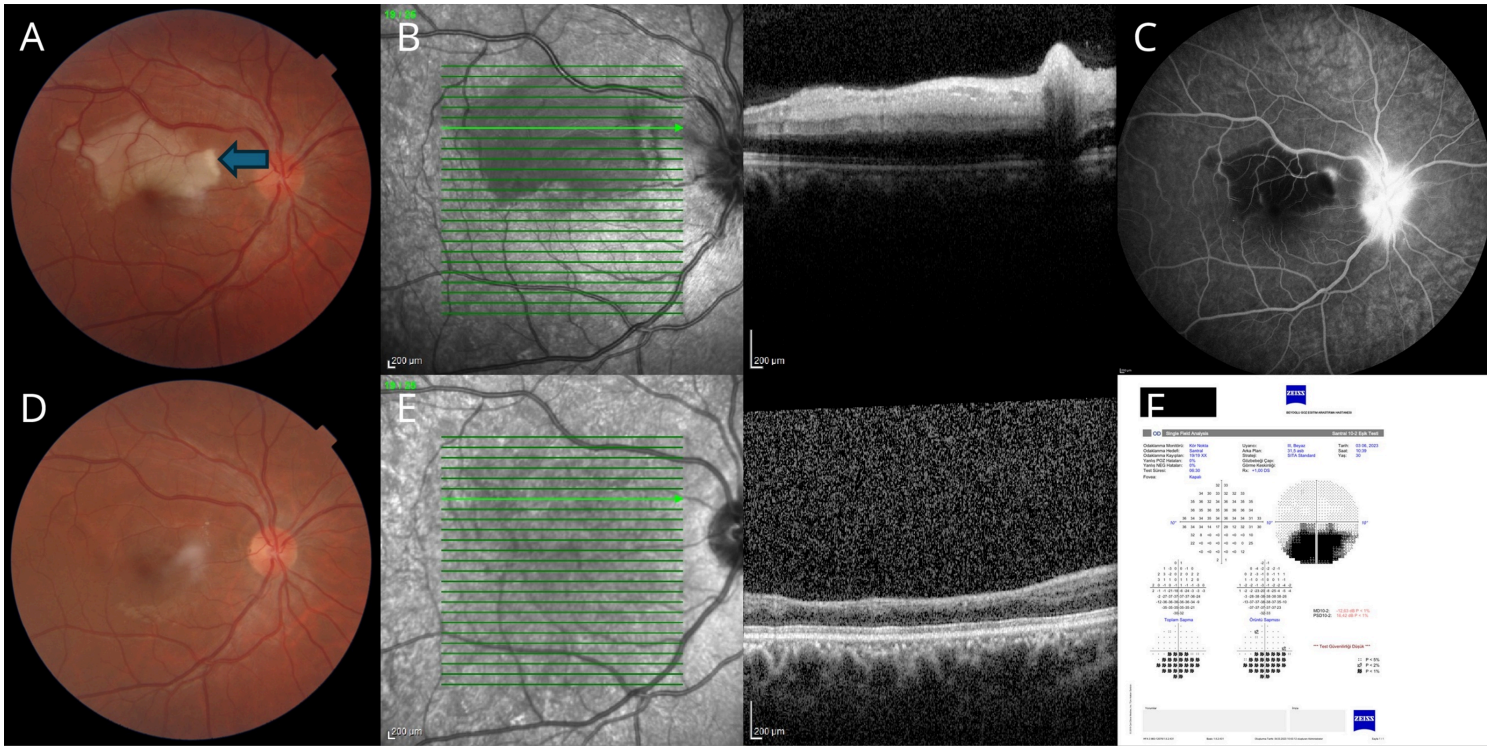


Figure 4

Fundus photography, infrared imaging, optical coherence tomography (OCT), fluorescein angiography, and visual field findings of a patient (Case 3) with superficial retinal infiltration associated with retinal arterial occlusion. At initial examination, color fundus photography shows a superficial retinal infiltrate (blue arrow) located superior to the fovea with an adjacent area of retinal whitening compatible with retinal arterial occlusion (A). Macular OCT B-scan through the lesion demonstrates inner retinal layer edema in the region of the arterial occlusion and retinal infiltration (B). A late-phase (10-minute) fundus fluorescein angiography image obtained at presentation is shown in (C). At the 1-year examination, color fundus photography shows resolution of the acute retinal findings (D), while the corresponding macular OCT B-scan demonstrates residual inner retinal layer atrophy in the area of the previous arterial occlusion (E). Automated visual field testing performed at the same visit reveals an inferior visual field defect corresponding to the affected retinal region (F).

Supplementary Files

This is a list of supplementary files associated with this preprint. Click to download.

- ESM1.xlsx